COBEM 2023 27TH INTERNATIONAL CONGRESS OF MECHANICAL ENGENEERING

ABCM Brazilian Society of Mechanical Sciences and Engineering
27th ABCM International Congress of Mechanical Engineering
December 04-08, 2023, Florianópolis-SC, Brazil

COB-2023-1487
INFLUENCE OF PRINTING PARAMETERS AND MEAN STRESS ON THE FATIGUE BEHAVIOR OF ABS SAMPLES OBTAINED BY FFF

Vinícius Hiroshi Souza Miwa
Universidade Federal de Goiás
vhiroshimiwa@gmail.com

Angélica Oliveira de Barcelos
Sergio Henrique da Silva Carneiro
Manuel Nascimento Dias Barcelos Júnior
Universidade de Brasília
angelicaoliveira.barcelos@gmail.com
shscarneiro@unb.br
manuelbarcelos@unb.br

Daniel Fernandes Da Cunha
Universidade Federal de Goiás
danielcunha@ufg.br

Abstract. *Fatigue fracture is a leading cause of mechanical failure, making it critical to understand the behavior of polymeric materials, particularly Acrylonitrile Butadiene Styrene (ABS), in this phenomenon. The objectives of this study were to develop and characterize printed ABS specimens using fused filament manufacturing with different filament directions and variations in printing parameters and to investigate the behavior of the material under mechanical fatigue. The study began by designing and printing the specimens using standardized methods. Static tests were then performed to characterize the material, including predicting the effect of mean stress using various methods such as Goodman, Soderberg, Gerber, and ASME Elliptical. To predict the stress-life (S-N) curve, a method based on Juvinall's approach was developed and evaluated. Finally, the mechanical response of specimens printed with different filament depositions was compared with results from tests performed previously. Among the methods used, the Gerber method proved to be the most effective in predicting the variation in fatigue life as a function of the mean stress. The method adapted from Juvinall also demonstrated a coherent approximation of the experimental result for predicting the S-N curve. However, the need to use Gerber during development was identified. The comparison of the specimens' mechanical response showed that those with filaments parallel to the load exhibited better results than perpendicular ones. Crossed filaments showed intermediate resistance, greater ease of printing for the body in question and appears to be a good approximation for an isotropic material. Nonetheless, the choice of orientation should consider the properties of each print. From the results, it was also possible to identify a significant variation in mechanical resistance depending on the printer and chosen to manufacture parameters. Furthermore, among the printing parameters evaluated, the only one that demonstrated relevance to the result was the internal padding. In conclusion, understanding the behavior of ABS in fatigue fracture is critical in many applications. This study provides a valuable contribution by characterizing the material, developing new methods for predicting its behavior, and comparing the effects of different filament orientations and other printing parameters on the mechanical response.*

Keywords: *FFF, 3D Printing, Fatigue, Fracture Mechanics*

1. INTRODUCTION

Mechanical fatigue is a fracture phenomenon that has been studied since the 19th century. This phenomenon has great effects in the field of Engineering. For the development of new structures, it must always be taken into account since it is one of the most important reasons for the mechanical failure of the material. It is estimated that 50% to 90% of the causes of mechanical failure are caused for Fatigue (da Rosa, 2002).

The use of new materials has grown in recent years, and materials such as polymers have gained space in the most diverse areas. The use of polymers can be mapped, for example, in the Automotive, Aerospace, and Biomedical industries, among others (Slaton, 2020).

However, a lower production of Fatigue jobs is noticeable compared to static tension. Probably due to the difficulty

of carrying out experiments in this area the time required for carrying out is much longer. This smaller amount of bibliography is aggravated in recent materials developed or that are in the process of being adopted by the industry. Thus, it becomes essential to study the phenomenon of Fatigue in polymers.

With this in mind, several authors have already sought to understand the effect of fatigue on polymers manufactured by fused filament manufacturing (FFF). Svetlana *et al.* (2021), for example, evaluated the behavior of polyamide 6 and polyamide 12 in bending tests in three-point bending in both fatigue and quasi-static conditions. She sought to understand the effect of porosity and the differences between materials. Paggi *et al.* (2019), in turn, employed bending tests, but their main objective was to examine the performance of cellulose tablets. They also investigated the influence of printing parameters, highlighting their relevance for biomedical applications.

Axial fatigue tests, as well as bending ones, have already been investigated by several authors. Polylactic acid (PLA) is one of the most used materials in FFF printing. Therefore, Gaweł *et al.* (2023) investigated the variation in density in test specimens produced from PLA by FFF. Meanwhile, Miller *et al.* (2017) was concerned with observing the behavior of polycarbonate urethane. He compared the material produced by FFF and that produced by injection molded sheets.

ABS polymer as it is one of the most used materials in FFF production, along with PLA, and there are several publications related to it. Several authors have investigated the effects of fatigue due to rotational bending stress on ABS, including Bagheri *et al.* (2022), Brčić *et al.* (2021), Azadi *et al.* (2021). Bagheri *et al.* (2022), focused the study on the PLA and ABS production process, he noticed that the non-welded specimens had a higher fatigue response than the others. Brčić *et al.* (2021) made a comparison between ABS, PLA, and acrylonitrile styrene acrylate (ASA). Azadi *et al.* (2021) compared ABS and PLA in different deposition directions, and he concluded that PLA has a superior response to ABS in rotational bending fatigue.

Finally, Jap *et al.* (2019) similar to this work, sought to understand ABS in axial fatigue. He compared a specimen with the filaments directed at -45º/45º (called 45º/135º in the present work) and another at 0º and 90º. He noticed that in static stresses both presented similar values, however, in fatigue the specimen at -45º/45º presented a 63.5% higher response.

From this, the present work aimed to adapt and validate the Juvinall method for predicting the SN curve for ABS material. In addition to comparing the different filament directions and printing parameters resulting from FFF to bring the material closer to isotropic behavior.

2. FUSED DEPOSITION MOLDING

Fused filament fabrication is the deposition of the material layer by layer to create 3D objects. The process is usually referred as "three-dimensional printing of continuous-fiber composites by in-nozzle impregnation" (Aliheidari *et al.*, 2017).

This manufacturing process creates a material that exhibits anisotropic behavior, which, due to the direction in which the filaments are placed, will behave differently (Ahn *et al.*, 2002).

A few factors may change the characteristics of the component. Some of them are the velocity of printing, the direction of deposition, and temperature.

3. MECHANICAL FATIGUE

In engineering, it is common to study stresses that the load is applied only once, that is, static loads. However, in real situations, it is commonplace for failure to be caused by loads much lower than the tensile strength, sometimes even lower than the yield stress. This is due to the continuous repetition of loads that weakens the material to the point of catastrophic rupture of the part, and this event is called Fatigue (Shigley *et al.*, 2011).

This cyclical behavior can be illustrated, as shown in the Fig. 1.

Some concepts are important for the development of the work:

σ_{min}: minimum stress;

σ_{max}: maximum stress;

In addition to minimum stress and maximum stress, the Eq. (1) to Eq. (4) are important parameters for characterizing Fatigue:

stress variation:

$$\Delta\sigma = \sigma_{max} - \sigma_{min}, \tag{1}$$

mean stress:

$$\sigma_m = \frac{\sigma_{max} + \sigma_{min}}{2}, \tag{2}$$

alternating stress:

$$\sigma_a = \frac{\Delta\sigma}{2}, \tag{3}$$

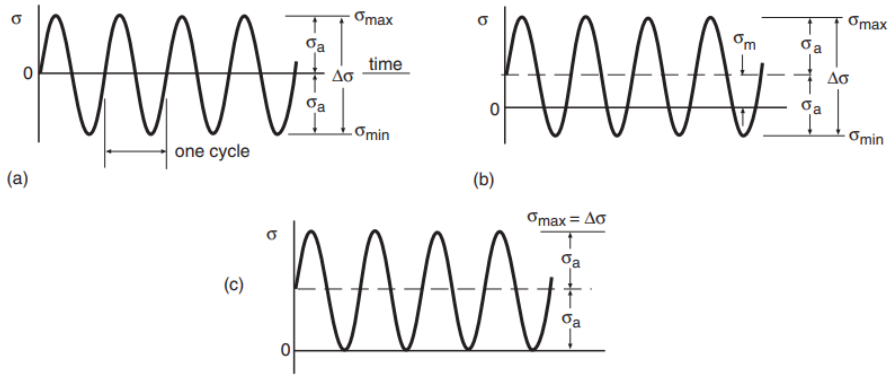

Figure 1. Nomenclature for constant amplitude cycling loading. Constant amplitude cycling and the associated nomenclature. Case (a) is completely reversed stressing, σ_m = 0; (b) has a nonzero mean stress σ_m; and (c) is zero-to-tension stressing, σ_{min} = 0. Source: Dowling (2013).

stress ratio:

$$R = \frac{\sigma_{min}}{\sigma_{max}}, \tag{4}$$

3.1 S-N curve

The German Engineer Friedrich Wöhler, through the study of fatigue in train axles, developed a relationship between stress and the number of cycles to failure. This relationship became known as the S-N curve (Suresh, 1998). An example of an S-N curve can be seen in Fig. 2.

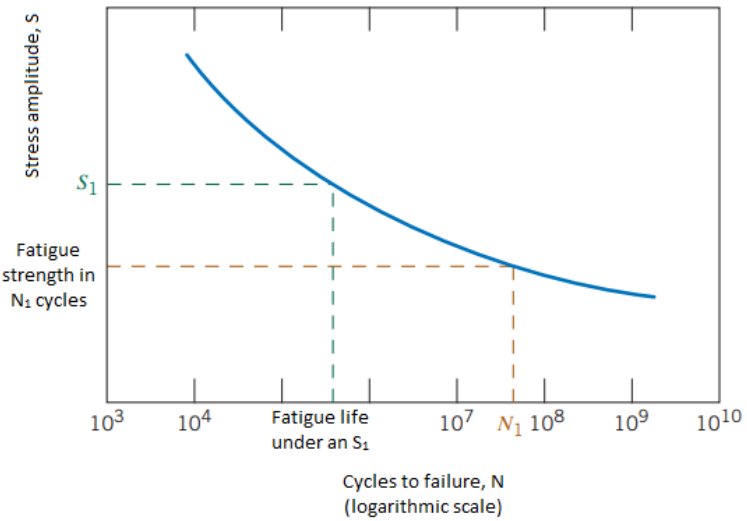

Figure 2. S-N curve. Source: adapted from Callister (2016).

This stress ratio per number of cycles is used to understand the behavior of the material and is therefore relevant for designing the period in which this material is capable of withstanding (Shigley *et al.*, 2011). As a result, there is a need to develop methods that predict this curve for the most different materials and stress ratios.

3.2 Effect of mean stress

The variation of mean stress can change the number of cycles before the failure of a component. To correct these changes produced by the effects of the mean stress, empiric methods based on experimental results were developed. The ones used in this paper are presented below in Eq. (5) to Eq. (8).

The Gerber method is the most conservative of them all, followed by Goodman, ASME Elliptical, and Soderberg Budynas *et al.* (2011). This, however, takes into account that the values are being calculated from R = -1 or σ_m = 0, which does not happen in the present work. Taking into account that the results originated from tests carried out by Pereira (2019), in which the R values are 0.1 and 0.3.

Goodman:

$$\frac{\sigma_{\mathbf{a}}}{\sigma_{\mathbf{ar}}} + \frac{\sigma_{\mathbf{m}}}{\sigma_{\mathbf{u}}} = 1, \tag{5}$$

Gerber:

$$\frac{\sigma_{\mathbf{a}}}{\sigma_{\mathbf{ar}}} + (\frac{\sigma_{\mathbf{m}}}{\sigma_{\mathbf{u}}})^2 = 1, \tag{6}$$

Soderberg:

$$\frac{\sigma_{\mathbf{a}}}{\sigma_{\mathbf{ar}}} + \frac{\sigma_{\mathbf{m}}}{\sigma_{\mathbf{0}}} = 1, \tag{7}$$

ASME Elliptical:

$$(\frac{\sigma_{\mathbf{a}}}{\sigma_{\mathbf{ar}}})^2 + (\frac{\sigma_{\mathbf{m}}}{\sigma_{\mathbf{0}}})^2 = 1, \tag{8}$$

Where:

- σ_a: alternate stress;
- σ_m: mean stress;
- σ_{ar}: stress amplitude when mean stress is equal to 0;
- σ_0: yield stress;
- σ_u: tensile strength.

3.3 Fatigue life prediction

The need to predict the mechanical behavior under fatigue led to the emergence of some methods for predicting the S-N curve, including the Juvinall method. Such a method is illustrated in Fig. 3.

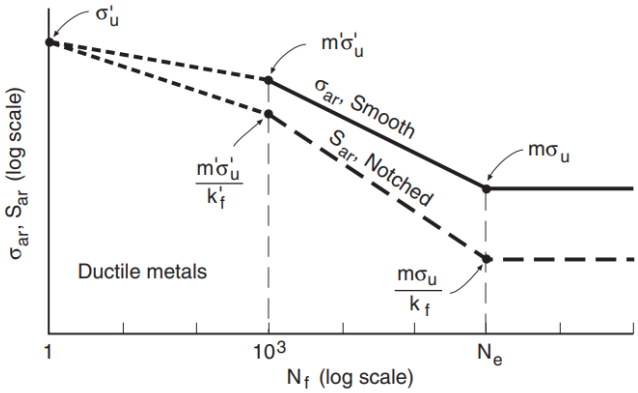

Figure 3. Estimating completely reversed S-N curves for smooth and notched members according to procedures suggested by Juvinall. Dource: Dowling (2013).

The prediction of the curve is based on 3 points that are estimated as a function of loading and material properties.

Since the first point is located at N = 1, this point is given by σ'_u, which is the resistance to tension or bending, or the maximum resistance in shear to torsion. In the present work, this value was considered equal to σ_u for simplification purposes and due to data and equipment limitations. The second point, located at 10^3, is calculated from, in addition to σ'_u, a constant m'. This constant depends on the loading conditions and the material. Finally, in the third and last point, located at N_e (a value that depends on the type of material and illustrates the point where the fatigue limit occurs), the factor m appears, which, similar to m', is a constant dependent on material type and loading. In the notched case, there are still two notch factors k'$_f$ and k$_f$; however, these values are not important for the present work, since this type of specimen was not used (Dowling, 2013).

4. METHODS

Initially, two specimens were developed. The first being oriented at 45°/135° and the second oriented at 0°/45°/90°/135°. These specimens were designed with the aim of bringing the material closer to isotropic behavior. It was hypothesized that a material that has a greater number of different angles, uniformly divided between 0° and 180°, would result in behavior closer to that seen in isotropic materials. These results were compared among themselves and between the values found by Miwa (2022) and Pereira (2019), all following ASTM D638 standard. Figure 4 shows the disposition of the filaments used by Miwa (2022) and of the present work, the filaments in 0°/45°/90°/135° have directed layers as illustrated by the a, c and d. It is worth mentioning that Pereira (2019) did not mention the direction of the filaments, it is believed that the d arrangement was used.

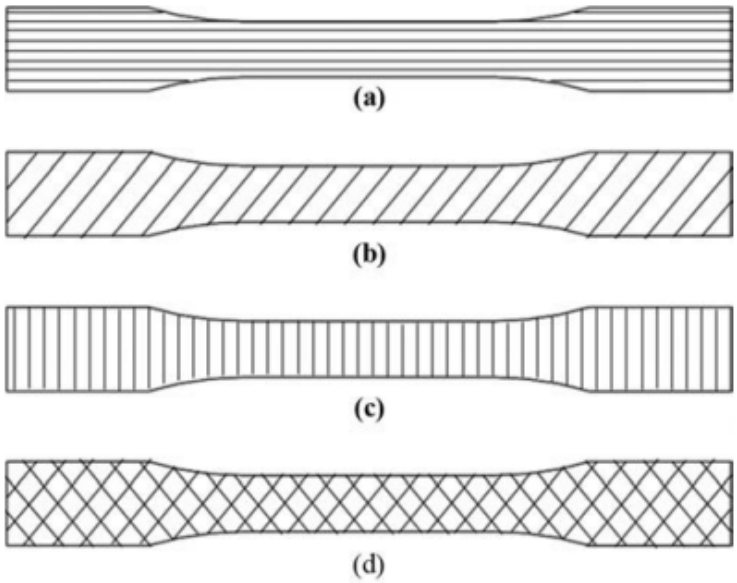

Figure 4. Filament orientations. (a) 0°, (b) 45°, (c) 90°, (d) 45°/135°. Source: Ziemian *et al.* (2015).

The printing parameters used in works can be viewed in the Tab. 1.

Table 1. Printing parameters.

Parameters	**Present Work**	**Pereira (2019)**	**Miwa (2022)**
Printing temperature, ºC	230	230	230
Internal padding, %	100	100	100
Maximum speed, mm/s	40	60	40
Contour overlay, %	84	-	84
Extrusion width, mm	0.39	-	0.39

The fatigue data from the Tab. 2 and Tab. 3, developed by Pereira (2019) following ASTM D7791, were used to make a comparison between the methods of incorporating the effect of mean stress. For that, the Eq. (5), Eq. (6), Eq. (7) and Eq. (8) were used for the results found in R = 0.1 by Pereira (2019) were taken up to the value of R = 0.3 and vice versa. In this way, it was possible to make a comparison between the calculated and experimental values and discover which of the methods best adapted to the ABS. Miwa (2022) carried out a similar analysis; however, a numerical approach was used, different from the present work that used analytical calculations.

Table 2. Alternating stress with R = 0.1. Source: adapted from Pereira (2019).

Ciclos	**Pereira (2019) (R = 0.1)**
2530	9.41
5347	8.37
9537	7.32
20868	6.27
40368	5.23

Table 3. Alternating stress with R = 0.3. Source: adapted from Pereira (2019).

Ciclos	Pereira (2019) (R = 0.3)
6078	7.32
13066	6.51
26055	5.69
51661	4.88

Therefore, the method most adapted to ABS was used to calculate the results of Pereira (2019) at R = -1, both for values at R = 0.1 and at R = 0.3. From this new curve calculated at R = -1, it was possible to develop a logarithmic trend line, also taking into account the point at N = 1, where $\sigma_{ar} = \sigma_u$ was used, as well as the Juvinall method suggests. This trend line was used to calculate the m and m' values.

From the values of m and m' it becomes possible to calculate the points of N = 10^3 and N_e, in addition to estimating S-N curves for the ABS as Juvinall's method suggests.

For the case of the article, a new trend line is drawn using this proposed method, being able, from it, to calculate values of σ_{ar} as a function of the number of cycles in fatigue for the ABS. This approach can also be seen in the work developed by Miwa (2022).

Using the proposed method, together with the data developed by caixeta and by miwa, in addition to those developed during the present work, it was possible to develop a comparison for the case of fatigue. The static properties found by Miwa (2022) and Pereira (2019) are listed in the Tab. 4.

Table 4. Properties of different filament directions. Source: adapted from Miwa (2022).

	Miwa (2022) 0°	Miwa (2022) 90°	Miwa (2022) 45°/135°	Pereira (2019)
E - elasticity modulus, GPa	2.31 ± 0.01	2.17 ± 0.01	2.22 ± 0.01	1.8 ± 0.05
σ_{bre} - breaking stress, MPa	25.82 ± 0.12	24.06 ± 0.73	25.75 ± 0.11	22.21 ± 0.88
σ_u - tensile strength, MPa	32.01 ± 0.06	24.50 ± 0.95	28.09 ± 0.27	23.24 ± 0.45
σ_0 - yield stress, MPa	31.85 ± 0.08	24.39 ± 0.86	27.62 ± 0.26	18.14 ± 0.44

Finally, a 2K factorial design was developed using Minitab software to understand the effects of printing parameters on loading, in addition to observing the approximation between the two filament direction arrangements. For this, only tensile strength was chosen, as data processing is not laborious and this parameter was consistent both in the tests Miwa (2022), Pereira (2019), and in those developed in the present work. To this end, the planning levels and parameter variations are explained in the Tab. 5.

Table 5. Printing parameters.

Level	Maximum speed	Internal padding	Filament directions	Temperature
Low	40 mm/s	80%	45°/135°	225ºC
High	60 mm/s	100%	0°/45°/90°/135°	230ºC

5. RESULTS AND DISCUSSION

The results found in the tensile test are statistically consistent. Therefore, the hypothesis that a greater number of angles of the filaments' directions would result in a better approximation to isotropy was not confirmed, as can be seen in Tab. 6.

Table 6. Properties of different filament directions.

	45°/135°	0°/45°/90°/135°
E - elasticity modulus, GPa	1.65 ± 0.03	1.69 ± 0,07
σ_{bre} - breaking stress, MPa	27.81 ± 1.00	27.74 ± 0.84
σ_u - tensile strength, MPa	31.74 ± 0.28	31.50 ± 0.62
σ_0 - yield stress, MPa	31.40 ± 0.37	30.93 ± 0.31

Note that in all tests, the same material and the same standard were used; in addition, Miwa (2022) used the same 3D printer as the present work. Even so, there were relevant differences in terms of results. This is probably due to the

tensile testing machine, which was the same only in the case of Miwa (2022) and Pereira (2019), and the software used for slicing the test specimens, which varied depending on the work. As can be seen in Fig. 5.

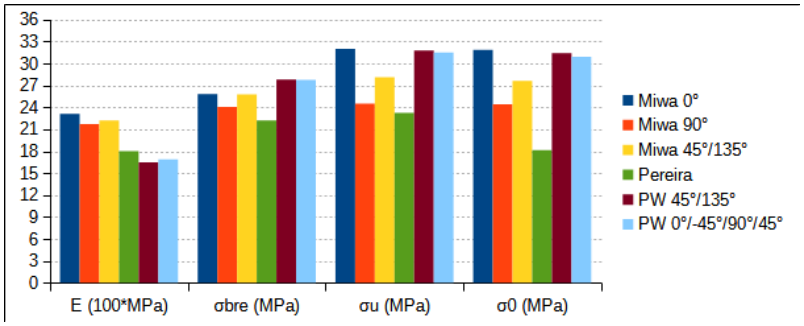

Figure 5. Comparison between different tests. PW - "present work"; Miwa - Miwa (2022); Pereira - Pereira (2019).

The method that showed the best approximation on the effect of mean stress was the Gerber method, followed by ASME Elliptical, which presented a similar approximation as can be seen from the Fig. 6.

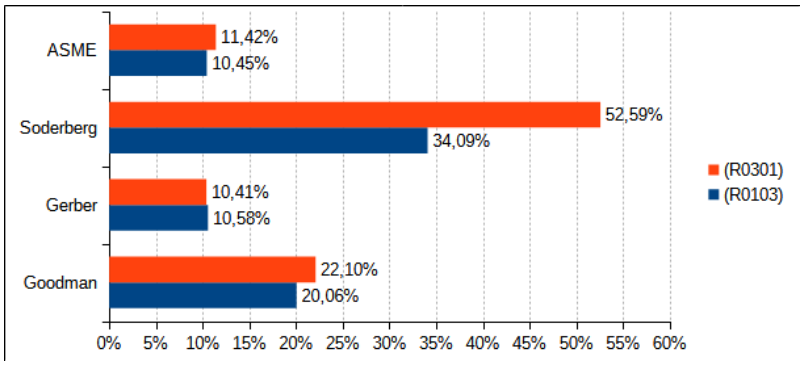

Figure 6. Mean error. R0301 is the stress at R = 0.3 calculated from R = 0.1; R0103 is the stress at R = 0.1 calculated from R = 0.3;

The proposed method presented an average error of 7.49%, taking into account that the adaptation of the Gerber method used to take the results up to $\sigma_m = 0$; therefore, it can be said that it is an acceptable approximation. The errors as a function of the number of cycles can be seen in Fig. 7 and Fig. 8.

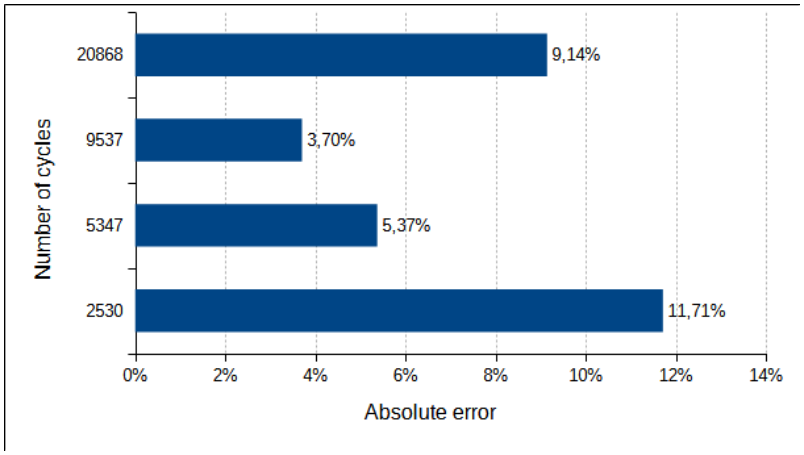

Figure 7. Absolute error of the proposed method at R = 0.1.

It is possible to see from Fig. 9 that the direction parallel to the load (0°) presented the best result, followed by 45°/135° and 90° to the tests developed by Miwa (2022). The PW and Miwa 0° values showed an almost overlapping; this is due to the dependence of the method on tensile strength; as these three models presented an approximate value, this is expected to happen.

The results obtained by the 2K factorial planning demonstrated a good fit and this can be seen in the Tab. 7.

The P-value demonstrates that the only relevant parameter for the case was internal filling, as the result is less than 0.05. It is noted that the directions of the filaments were not relevant in the case of 45°/135° and 0°/45°/90°/135°, but it

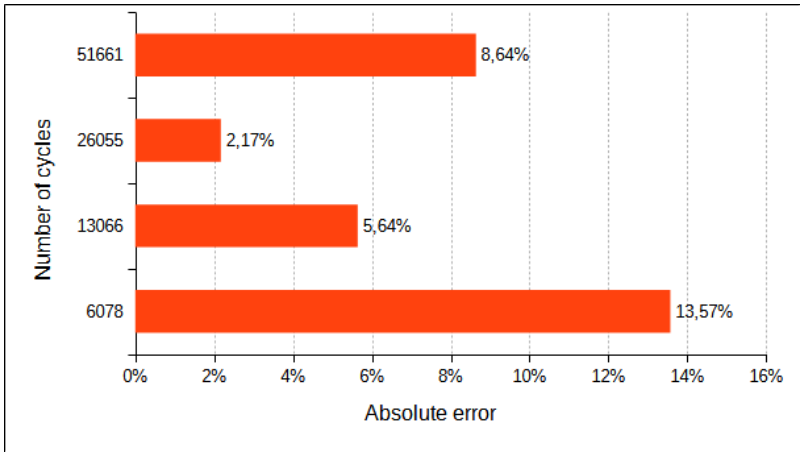

Figure 8. Absolute error of the proposed method at R = 0.3.

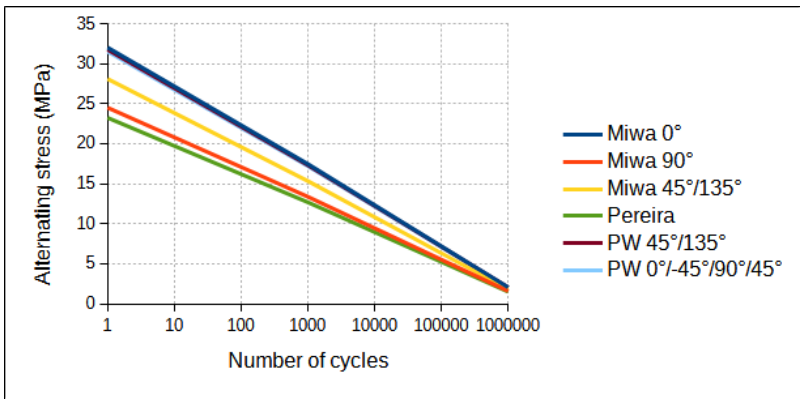

Figure 9. Comparison between filament directions

Table 7. Printing parameters.

S	R-squared	R-squared (adjusted)	R-squared (predicted)
0.901546	95.64%	86.93%	55.37%

cannot be said that the fatigue values are also equal as was demonstrated by Jap *et al.* (2019) that even if static values are close, differences in fatigue may be relevant. Furthermore, it is important to note that maximum speed and temperature were also not relevant for charging. As can be seen in the Tab. 8.

The residuals demonstrated a normal distribution, as expected, as can be seen in the Fig. 10.

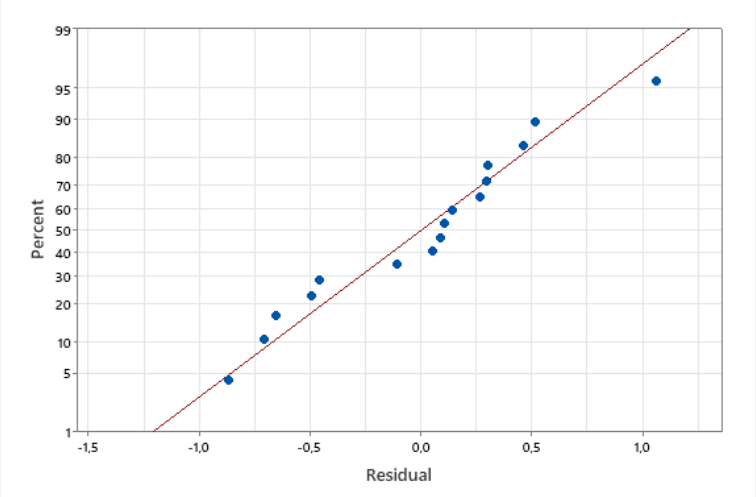

Figure 10. Residual

Table 8. Analysis of Variance.

Source	DF(1)	Adj SS(2)	Adj MS(3)	F-Value	P-Value
Model	10	89.1845	8.9184	10.57	0.008
Linear	4	87.3277	21.8319	26.86	0.001
Maximum speed	1	1.7292	1.7292	2.13	0.204
Internal padding	1	83.8140	83.8140	103.12	0.000
Filament directions	1	1.7292	1.7292	2.13	0.204
Temperature	1	0.0552	0.0552	0.07	0.805
2-Way Interactions	6	1.8567	0.3095	0.38	0.864
Maximum speed*Internal padding	1	0.8930	0.8930	1.10	0.343
Maximum speed*Filament directions	1	0.4160	0.4160	0.51	0.506
Maximum speed*Temperature	1	0.0992	0.0992	0.12	0.741
Internal padding*Filament directions	1	0.0020	0.0020	0.00	0.962
Internal padding*Temperature	1	0.0042	0.0042	0.01	0.945
Filament directions*Temperature	1	0.4422	0.4422	0.54	0.494
Error	5	4.0639	0.8128		
Total	15	93.2484			

(1) DF - degrees of freedom (2) ADJ SS - adjustes sum of squares (3) ADJ MS - adjusted mean of square.

6. CONCLUSIONS

The tensile tests demonstrated that a material behavior close to isotropic can be achieved from a 45°/135° disposition of the filaments. In addition, differences in test conditions were shown to be of great importance for the results.

It is concluded that the method that investigates the effect of the mean stress that best adapts to the ABS is the Gerber method. However, this method should be investigated starting from a mean stress equal to zero since, in a real situation, values that are lower than the experimental one can result in unexpected fractures, and the case of R0301, this was what happened. The hypothesis is raised that when the values are worked from a smaller R towards a larger one, this is not a problem since, in R0103, the values were higher than the experimental one.

The proposed method, adapted from Juvinall, showed very satisfactory results, even taking into account the Gerber method. However, this method presented some lower results than the experimental ones, which can result in unexpected fractures; therefore, high safety coefficients must be considered in the calculation. It is noteworthy that the script used to develop the method for ABS can be used for other materials. Finally, it is worth suggesting a work in which fatigue tests are carried out with the mean stress equal to zero. In this way, it becomes possible to develop the coefficients of the method without depending on the errors as a function of Gerber.

It was already expected that the fatigue results would follow the static results, and this is what happened when comparing the results of the filament directions. As can be seen, the directions of the filaments parallel to the load had a greater capacity to resist than the others, and this happens, probably due to the difficulty in breaking the parallel filaments in relation, for example, to breaking the junctions between the filaments of the body perpendicularly oriented test. In the case of 45°/135°, something similar happens; the filaments are able to resist partially compared to 0°.

Finally, the 2K factorial design was useful to confirm the hypothesis of approximation of the values of the arrangements at 45º/135º and 0º/45º/90º/135º. This reinforces that the 45º/135º direction is a good approximation of an isotropic material for the case of static loading. For fatigue, it must be tested experimentally, as the crack growth process can be influenced by the internal arrangement of the print. Furthermore, in the range studied, both maximum speed and temperature were not relevant to the response. This way, you can increase printing speed in a shorter time and reduce the temperature to save energy. It should also be noted that the internal filling of the impression is extremely important for the resistance of the specimen, taking into account its relevance to the result. This is explained by the density of the material, in addition to stress concentrators and failures that may arise due to the interfaces and voids between the filaments.

7. REFERENCES

Ahn, S.H., Montero, M., Roundy, D.O.S. and Wright, P.K., 2002. "Anisotropic material properties of fused deposition modeling abs". *Emerald insight*.

Aliheidari, N., Tripuraneni, R., Ameli, A. and Nadimpalli, S., 2017. "Fracture resistance measurement of fused deposition modeling 3d printed polymers". *Polymer Testing*, Vol. 60, pp. 94–101.

Azadi, M., Dadashi, A., Dezianian, S., Kianifar, M., Torkaman, S. and Chiyani, M., 2021. "High-cycle bending fatigue properties of additive-manufactured abs and pla polymers fabricated by fused deposition modeling 3d-printing". *Forces in Mechanics*, Vol. 3, p. 100016.

Bagheri, A., Parast, M.S.A., Kami, A., Azadi, M. and Asghari, V., 2022. "Fatigue testing on rotary friction-welded joints between solid abs and 3d-printed pla and abs". *European Journal of Mechanics-A/Solids*, Vol. 96, p. 104713.

Brčić, M., Kršćanski, S. and Brnić, J., 2021. "Rotating bending fatigue analysis of printed specimens from assorted polymer materials". *Polymers*, Vol. 13, No. 7, p. 1020.

Budynas, R.G., Nisbett, J.K. *et al.*, 2011. *Shigley's mechanical engineering design*, Vol. 9. McGraw-Hill New York.

Callister, W., 2016. *Ciência E Engenharia de Materiais: Uma Introdução* . Grupo Gen-LTC.

da Rosa, E., 2002. *Análise da Resistência Mecânica - Mecânica da Fratura e Fadiga*. Universidade Federal de Santa Catarina, Santa Catarina - Brasil.

Dowling, N.E., 2013. *Mechanical Behavior of Materials*. Pearson, Blacksburg, Virginia, Estados Unidos da América.

Gaweł, A., Kuciel, S., Liber-Kneć, A. and Mierzwiński, D., 2023. "Examination of low-cyclic fatigue tests and poisson's ratio depending on the different infill density of polylactide (pla) produced by the fused deposition modeling method". *Polymers*, Vol. 15, No. 7, p. 1651.

Jap, N.S., Pearce, G.M., Hellier, A.K., Russell, N., Parr, W.C. and Walsh, W.R., 2019. "The effect of raster orientation on the static and fatigue properties of filament deposited abs polymer". *International Journal of Fatigue*, Vol. 124, pp. 328–337.

Miller, A.T., Safranski, D.L., Smith, K.E., Sycks, D.G., Guldberg, R.E. and Gall, K., 2017. "Fatigue of injection molded and 3d printed polycarbonate urethane in solution". *Polymer*, Vol. 108, pp. 121–134.

Miwa, V.H.S., 2022. "Análise numérica e experimental da vida em fadiga do polímero acrilonitrila butadieno estireno impresso em 3d". *Universidade de Brasília*.

Paggi, R.A., Salmoria, G.V., Ghizoni, G.B., de Medeiros Back, H. and de Mello Gindri, I., 2019. "Structure and mechanical properties of 3d-printed cellulose tablets by fused deposition modeling". *The International Journal of Advanced Manufacturing Technology*, Vol. 100, pp. 2767–2774.

Pereira, F.C., 2019. "Caracterização do comportamento em fadiga do plástico abs produzido por extrusão e manufatura aditiva". *Universidade de Brasília*.

Shigley, J.E., Budynas, R.G. and Nibesett, J.K., 2011. "Elementos de máquinas de shigley". *AMGH Editora Ltda, 8ª ed, São Paulo, Brasil*.

Slaton, A.E., 2020. *New Materials: Towards a History of Consistency*. Lever Press, Amherst, Massachusetts. ISBN 9781643150130.

Suresh, S., 1998. *Fatigue of materials*. Cambridge university press.

Svetlana, T., Tatiana, T., Sergei, E., Innokentiy, S., Laurent, G. and Lamine, H., 2021. "Flexural quasi-static and fatigue behaviours of fused filament deposited pa6 and pa12 polymers". *The International Journal of Advanced Manufacturing Technology*, Vol. 117, No. 7-8, pp. 2041–2048.

Ziemian, S., Okwara, M. and Ziemian, C.W., 2015. "Tensile and fatigue behavior of layered acrylonitrile butadiene styrene". *Rapid Prototyping Journal*.

8. RESPONSIBILITY NOTICE

The authors are solely responsible for the printed material included in this paper.